Use of Computed X-Ray Tomographic Data for Analyzing the Thermodynamics of a Dissociating Porous Sand/Hydrate Mixture

Barry M. Freifeld[(1)]*, Timothy J. Kneafsey[(1)], Liviu Tomutsa[(1)], Laura A. Stern[(2)] and Stephen H. Kirby[(2)]

[(1)]Lawrence Berkeley National Laboratory, One Cyclotron Rd., Berkeley, CA. 94720, USA.
[(2)]U.S. Geological Survey, 345 Middlefield Rd., Menlo Park, CA. 94025, USA.

X-ray computed tomography (CT) is a method that has been used extensively in laboratory experiments for measuring rock properties and fluid transport behavior. More recently, CT scanning has been applied successfully to detect the presence and study the behavior of naturally occurring hydrates. In this study, we used a modified medical CT scanner to image and analyze the progression of a dissociation front in a synthetic methane hydrate/sand mixture. The sample was initially scanned under conditions at which the hydrate is stable (atmospheric pressure and liquid nitrogen temperature, 77 K). The end of the sample holder was then exposed to the ambient air, and the core was continuously scanned as dissociation occurred in response to the rising temperature. CT imaging captured the advancing dissociation front clearly and accurately. The evolved gas volume was monitored as a function of time. Measured by CT, the advancing hydrate dissociation front was modeled as a thermal conduction problem explicitly incorporating the enthalpy of dissociation, using the Stefan moving-boundary-value approach. The assumptions needed to perform the analysis consisted of temperatures at the model boundaries. The estimated value for thermal conductivity of 2.6 W/m K for the remaining water ice/sand mixture is higher than expected based on conduction alone; this high value may represent a lumped parameter that incorporates the processes of heat conduction, methane gas convection, and any kinetic effects that occur during dissociation. The technique presented here has broad implications for future laboratory and field testing that incorporates geophysical techniques to monitor gas hydrate dissociation.

Introduction

X-ray computed tomography (CT) has been applied by various researchers to visualize methane hydrates (Uchida, 2000, Mikami, 2000). Recently, Tomutsa et al. (2002) have shown that CT can be used to track (temporally and spatially) the progression of a dissociation front in a hydrate/sand sample. The objective of this paper is to demonstrate the use of CT, along with simple thermodynamic assumptions, to estimate the thermal conductivity that accompanies the complex mass and heat transfer processes associated with hydrate dissociation in a hydrate/sand system. Properties of pure methane hydrate have been studied in the laboratory, and the basic thermodynamic properties, including phase stability, heat capacity, and thermal conductivity, have been quantified over a significant range of temperatures and pressures (Sloan, 1998). However, extrapolating thermodynamic properties to methane hydrate within a natural porous formation remains a formidable challenge. Theoretical models for mixed systems abound, but actual data for hydrate/sand systems are very sparse. Estimates of the bulk heat capacity may be obtained by summing the heat-capacity contributions from the individual phases as long as such estimates suitably incorporate the strong dependence of heat capacity on temperature. Thermal conductivity, however, is dependent not just upon the intrinsic conductivity of the individual phases, but also a function of the thermal resistances across grain contacts, properties that depend on the quality, areas and geometry of such contacts. When complex processes such as hydrate dissociation and advective transport occur, estimating heat transport properties and the migration rates of phase boundaries is challenging and the required data and insight for modeling is lacking.

This paper uses a moving-boundary-value model, attributed to J. Stefan for his work on modeling melting of polar ice caps and icebergs in the 1890s. Here we apply a moving-boundary-model to interpret acquired CT data that tracks the time-dependent progression of a dissociation front in a cylindrical sand/hydrate sample. Only simple assumptions of constant boundary temperatures are required to apply the model. Previous researchers (Selim and Sloan, 1985, Ahmadi et al., 2000, and Tsypkin, 2000) have suggested the applicability of the moving-boundary-value problem to model hydrate dissociation, but have not provided any actual data. The ability for CT to track the time dependent progression of the hydrate dissociation front has provided an opportunity for direct application of a moving-boundary-value simulation. Although the model explicitly accounts for heat conduction with phase

* Corresponding author. E-mail: bmfreifeld@lbl.gov

change, the thermal conductivity value that is estimated represents a lumped parameter, combining heat transport resulting from both thermal conduction and nondiffusive transport, such as energy transport by advected gas and any potential kinetic effects.

Stefan problems have been solved analytically, without recourse to numerical techniques, for only a few simple geometries. The one-dimensional model used herein is applicable to a semi-infinite domain, and hence represents a simplification of the actual finite-length experimental system. To avoid the inaccuracies caused by the application of an infinite domain solution to modeling a finite-length experiment, only early time CT data were used. Clearly, additional interpretation of the complete data set is possible using numerical techniques. However, the primary value of the experiment presented is the development of a testing and thermodynamic analysis methodology that can be used for further laboratory study using CT. In addition, field experiments using noninvasive geophysical techniques to track a hydrate dissociation front, along with measurements of formation pressure, temperature and composition derived from well logs, can use Stefan problem solutions to estimate formation thermodynamic parameters. A better understanding of the thermodynamics of dissociation in mixed media can lead to an understanding of the complex coupled processes that govern any potential economic extraction of methane hydrates.

Experiment Description

The 2.54 cm diameter, 6.3 cm long porous methane hydrate/sand sample used in the experiment had a high initial porosity of 49%. The sample was a heterogeneous composite, with the upper half of the sample 60%/40% sand/hydrate (by solids volume), and the lower half 40%/60% sand/hydrate (by solids volume). The sample represents the middle portion of the hydrate/sand composite shown in Figure 1b. The sample was synthesized by combining cold, pressurized CH_4 gas (250 K, 27 MPa) with mixtures of sand and granular H_2O ice "seeds" (typically 26 to 32 g, at 180–250 μm grain size) in stainless steel reaction vessels. Upon heating and subsequent cooling the ice grains undergo conversion to hydrate grains by the general reaction CH_4 (g) + 5.9 H_20 (s→l) → CH_4·5.9 H_2O. The detailed procedure for forming the hydrate/sand sample used here is described in Stern et al. (1996) and Tomutsa et al. (2002).

The sample was placed in a gas-tight PVC sample holder with plastic fittings. The sample holder top was connected to a gas collection system. A sheathed type-J thermocouple was inserted through the sample holder bottom such that the sample would rest in contact with the thermocouple tip. The sample holder was set into an insulating Styrofoam container. These materials selected to contain the sample exhibit minimal x-ray attenuation, thus maximizing sensitivity of the CT to sample attenuation changes. A Siemens Somaton HiQ medical CT scanner was used to obtain the x-ray CT data. Axial cross sections 1 mm thick were obtained by scanning the vertically oriented sample with an x-ray energy of 133 keV and a current of 120 mA. The duration of each scan was 4 seconds. The voxel size (CT volume element) in each image was 1 mm × 0.2 mm × 0.2 mm. Initial scans were performed with the sample fixed at 77 K, using liquid nitrogen in the Styrofoam container. Scans of a near-center plane were performed to monitor sample changes over time. Time intervals between the scans varied from a few minutes (during pre- and post-dissociation phases) to a few tens of seconds (during the hydrate dissociation phase).

Scans were performed while allowing the nitrogen to boil off. When sufficient nitrogen had evaporated, the temperature at the sample bottom began to increase. We continued to scan the sample as the temperature increased and hydrate dissociation commenced. The volume of the gas evolved from the sample was measured by collection in a calibrated Mariotte bottle. Displaced water from the Mariotte bottle was captured in a reservoir that was continuously weighed. The composition of the gas was measured following dissociation, using a LandTec GEM 2000 landfill gas analyzer.

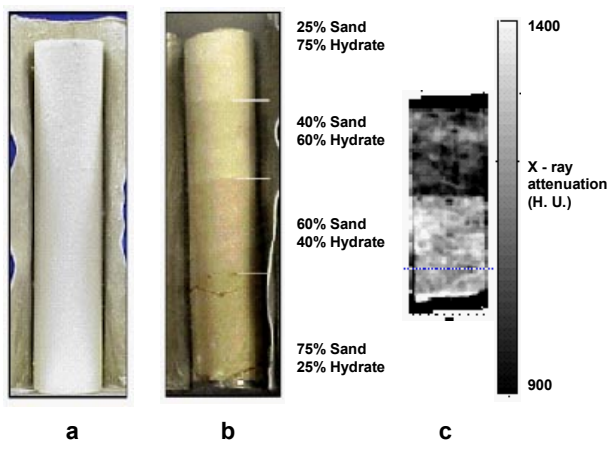

Figure 1. Synthetic methane hydrate samples and an x-ray image: (a) pure hydrate, (b) composite with sand, (c) baseline x-ray CT image of mid-portion of sand/hydrate composite as used in the dissociation-front tracking experiment.

Experiment Results

Initially, the sample was maintained within the stability region of the methane hydrate at the nitrogen boiling point (77 K, 0.1 MPa) to establish a baseline CT attenuation data set. As the temperature of the sample increased by thermal conduction above 77 K, but still

within the stability region of the methane hydrate, we noted reductions in beam attenuation that coincided with the evolution of gas into the Mariotte bottle. We interpreted this as indicating the presence of nitrogen within the sample, which was subsequently confirmed with the chemical analysis of the evolved gas. The scan taken immediately after the bulk of the liquid nitrogen was determined to have boiled off (shown in Figure 1c) was used as a baseline for comparison with subsequent scans. By differencing the subsequent scans with the baseline data, hydrate dissociation could easily be detected by resolving the advancing dissociation front. Figure 2 presents the CT data for a few selected CT scans that were differenced with the baseline image. The downward movement of a region of decreased attenuation delineates the vertically propagating dissociation front. The movement of the front is also presented in Figure 3, where the lateral average of x-ray attenuation of a vertical central band, equal to the length of the sample and 60% of its width (shown as a box in the first image of Figure 2), was plotted over the duration of the experiment using all the CT scans. The change in attenuation caused by the advancing dissociation front is seen as a curve between regions of different attenuation.

In addition to x-ray attenuation changes, Figure 3 also shows the temperature at the bottom of the sample over the duration of the experiment. Initially, the sample contained liquid nitrogen at the bottom and remained at the normal boiling point. During this time period, liquid nitrogen was also applied in the Styrofoam container to cool the sample holder and sample. When the liquid nitrogen in the sample boiled off, the temperature initially increased fairly uniformly at a rate of about 1.2°C/min, but gradually declined to a rate of 0.9°C/min.

The gas production curve overlies the CT data in Figure 3. For the first 90 minutes of the experiment, gas was generated at about 6.4 ml/min. We attributed this primarily to the release of adsorbed nitrogen gas. After 90 minutes, a marked increase in gas production was observed (to about 23.5 mL/min). After about 124 minutes, the rate again increased (to about 31.8 mL/min) even with a lower rate of temperature increase. The total gas produced prior to 90 minutes was about 370 mL. By 124 minutes, an additional volume of 790 mL was produced, and after 124 minutes 590 mL of gas was produced. A total of 1120 mL of methane and 630 mL of nitrogen were produced (at room temperature and pressure). This implies that about 0.75g (~1 mL liquid if in that form) of nitrogen was initially present. The volume of nitrogen ultimately produced significantly exceeds the amount of nitrogen produced when the temperature first exceeded the nitrogen boiling point (~260 mL), indicating that nitrogen was present in a significant quantity but apparently not in free liquid or gas form. Although we suspect the nitrogen is adsorbed, it is not entirely clear when during the experiment it entered the collection bottle. We attribute the nitrogen collected to the long duration (greater than 1 year) during which the sample was stored in liquid nitrogen.

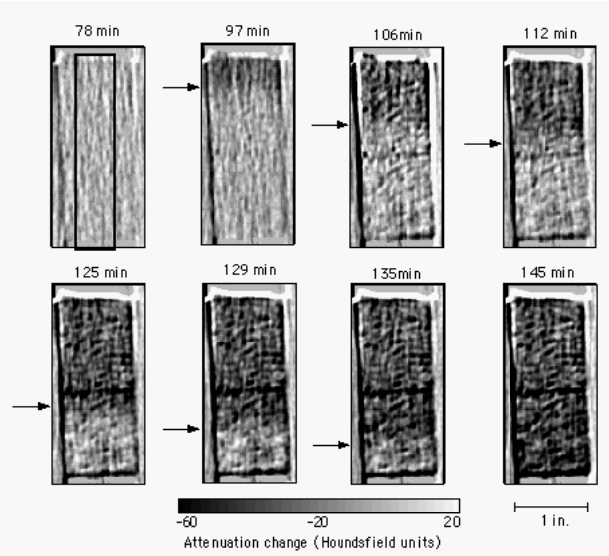

Figure 2. X-ray CT images showing attenuation changes as the dissociation front progresses downward in the methane hydrate sample. Images have been differenced from an initial baseline image. Arrows show location of the dissociation front.

Mathematical Model

The movement of the dissociation front in the sand/hydrate system can be modeled as a classical Stefan moving-boundary-value problem, a general class of diffusion problems in which a medium exhibits a discontinuity that moves in response to or because of diffusion. Crank (1985) presented Neumann's solution to the Stefan problem for the progressive freezing of a liquid caused by heat extracted from a fixed boundary in a semi-infinite one-dimensional domain. In the ice-liquid system, the phase transformation at the moving boundary is explicitly accounted for by incorporating the heat of fusion in the energy balance for the system. The mathematic problem of dissociation of methane hydrate into ice water and methane is analogous, with the addition of heat at the fixed boundary. The latent heat associated with the hydrate phase change at the moving boundary is therefore explicitly accounted for in the system energy balance. Figure 4 shows the model schematically incorporating a moving hydrate/ice interface, along with the assumed temperature boundary conditions. Table 1 shows the assumed thermodynamic properties in the model. Note that heat capacity is strongly dependent on temperature, and hence a value was chosen representative of the average experimental temperatures, midway between the two extremes of 77 K and 273 K.

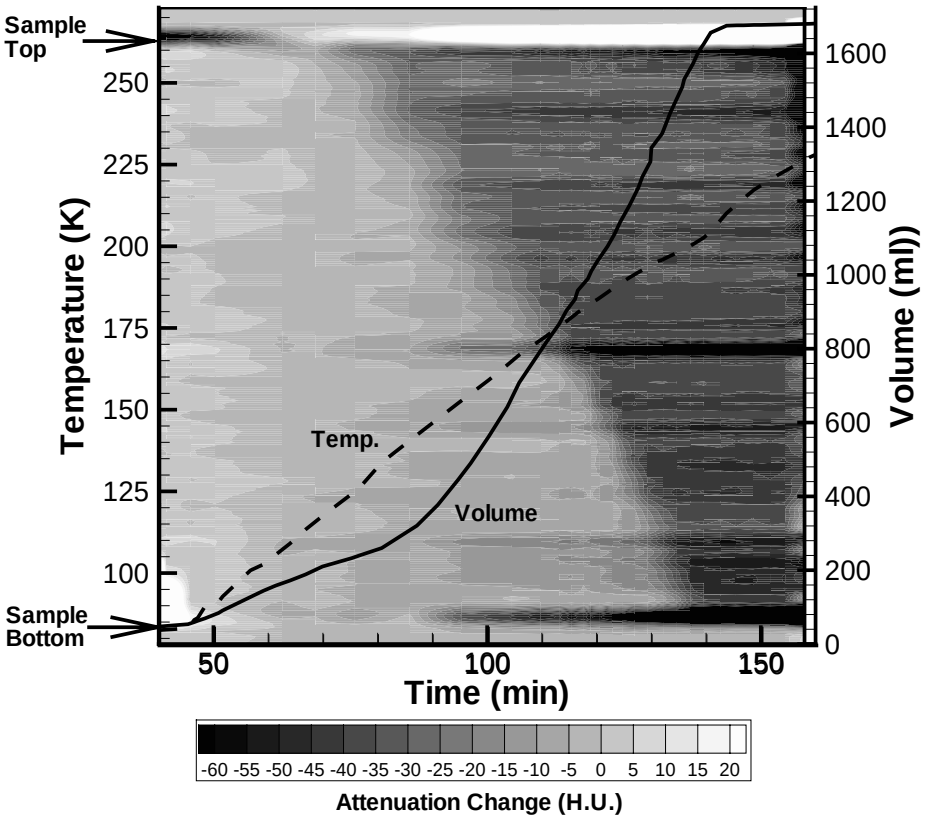

Figure 3. Composite image of an averaged vertical slice from the x-ray CT images of the methane hydrate sample, showing the dissociation front (noted by the steep change in attenuation) progressing downward. Superimposed over the image is the total volume of gas evolved and the temperature at the bottom of the sample.

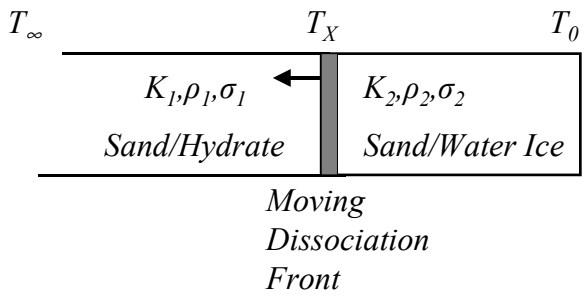

Figure 4. Schematic illustration of the Stefan moving-boundary-value problem incorporating hydrate phase change. The temperature of the hydrate is initially at T_∞ throughout the semi-infinite domain. T_X is the dissociation temperature and the temperature at the fixed end is maintained at T_0 for all times.

Table 1. Thermodynamic Properties Assumed in the Hydrate Dissociation Model

Material	Heat Capacity (J/gK) σ	Density (g/cm^3) ρ	Enthalpy of Dissociation (to Water Ice+CH_4) (J/g) ΔH
Quartz	0.6	2.65	
Hydrate	1.8	0.92	1.137×10^3
Porous Ice*	2.1	0.80*	

* Porous ice represents water ice plus added gas filled pore space, which assumes that the bulk structure of the hydrate ice is not rearranged upon dissociation. Actual ice grain density is higher.

With the experimental data set collected, we estimate a lumped heat transfer parameter for the sand/water ice plus evolved methane gas system. We refer to this parameter as the thermal conductivity of the sand/water ice medium, but recognize that it incorporates not only conductive but also advective transport of energy and any additional kinetic effects. We chose a thermal conductivity of the hydrate/sand mixture based upon measurements performed by Waite (2002). His measurements of thermal conductivity of a 60% sand/40% hydrate system, using the needle probe method of von Herzen and Maxwell, suggests a thermal conductivity of 0.9 W/mK. This value represents a purely conductive process, with no phase change or advective transport.

To set up the heat conduction problem we set the initial temperature throughout the semi-infinite domain, T_∞, to the boiling point of liquid nitrogen, 77 K. T_0 is the temperature maintained at the surface through which heat is added, 273 K, the melting point of water ice. T_x, the temperature that methane hydrate dissociates at 0.1 MPa, was chosen as 200 K, based upon an inflection in the temperature time history shown in Figure 3. This temperature is greater than the stability temperature (193 K, 0.1 Mpa), but according to Stern et al. (2001), it is a temperature at which dissociation has been shown to proceed rapidly. The solution to the one-dimensional heat flow problem as given by Crank (1985) is

$$\frac{\sigma_1(T_\infty - T_x)}{f\left(\beta/D_1^{1/2}\right)} + \frac{\sigma_2(T_0 - T_x)}{g\left\{\rho_1\beta/\left(\rho_2 D_2^{1/2}\right)\right\}} + \Delta H = 0 \qquad (1)$$

where f and g are the functions

$$f\left(\frac{\beta}{D_1^{1/2}}\right) = \pi^{1/2}\frac{\beta}{D_1^{1/2}}\exp\left(\beta^2/D_1\right) erfc\frac{\beta}{D_1^{1/2}} \qquad (2)$$

$$g\left(\frac{\rho_1\beta}{\rho_2 D_2^{1/2}}\right) = \pi^{1/2}\frac{\rho_1\beta}{\rho_2 D_2^{1/2}}\exp\left(\rho_1\beta^2/\rho_2^2 D_2\right) erf\frac{\rho_1\beta}{\rho_2 D_2^{1/2}} \qquad (3)$$

ΔH is the enthalpy of dissociation. Here σ_1 and σ_2 represent the heat capacity of the lumped system of sand/hydrate and sand/water ice respectively. Similarly, ρ_1 and ρ_2 represent the density of the lumped system of sand/hydrate and sand/water ice. D_1 and D_2 represent the thermal diffusivity of the sand/hydrate and sand/water ice mixtures respectively, given the thermal conductivities K_1 and K_2, where

$$D_x = K_x/(\rho_x\sigma_x) \qquad (4)$$

The constant β is determined by looking at the location of the dissociation front, X, at time t using the relationship

$$\beta = \frac{X}{2t^{1/2}}\frac{\rho_2}{\rho_1} \qquad (5)$$

For the 60% sand/40% hydrate mixture used in this experiment, a bulk density of 0.963 g/cm^3 is calculated with a heat capacity of 0.792 J/gK. Upon dissociation, the sand/water ice mixture is computed to have a bulk density of 0.939 g/cm^3 with a heat capacity of 0.854 J/g K. This calculation assumes that there is no rearrangement of the sand matrix upon dissociation. The analytical model assumes that the low temperature boundary extends to infinity. In reality, the sample is only 6.3 cm long, and hence the model is only applicable to analyzing early time data. Figure 5 shows the temperature T_2 in the sand/water ice mixture computed using (Crank, 1985)

$$T_2 = T_x - (T_x - T_0)\left[1 - \frac{erf\left\{x_2/2(D_2 t)^{1/2}\right\}}{erf\left\{\rho_1\beta/\left(\rho_2 D_2^{1/2}\right)\right\}}\right] \qquad (6)$$

while the temperature in the sand/hydrate, T_1, is computed as

$$T_1 = T_x - (T_x - T_\infty)\left[1 - \frac{erfc\left\{x_1/2(D_1 t)^{1/2}\right\}}{erfc\left\{\beta/\left(D_1^{1/2}\right)\right\}}\right] \qquad (7)$$

Here x_1 (Equation 7) is valid at all locations greater than X, and x_2 (Equation 6) is valid between 0 and X, resulting in the temperature curves exhibiting a change in slope at the dissociation point, T=200 K. From the temperatures shown in Figure 5, we can see that the actual sample length (6.3 cm) becomes significant when the temperature at that location rises significantly above T_∞, between 200 and 1000 seconds after the sample initially begins dissociating.

Equation (1) was solved for K_2, the thermal conductivity of the sand/water ice mixture, and yielded

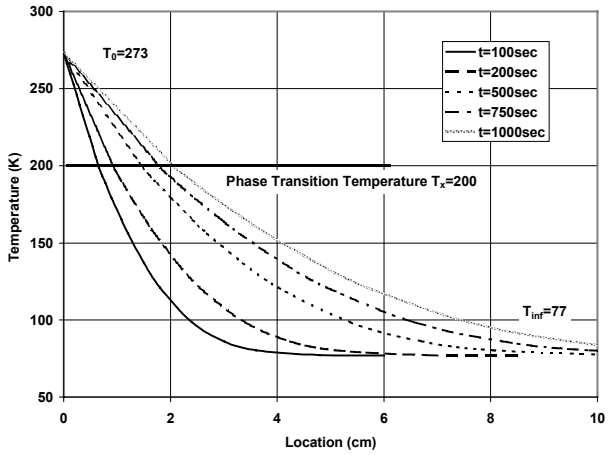

Figure 5. The progression of heating of a sand/hydrate sample modeled as a one-dimensional moving boundary problem incorporating phase change to ice water and methane gas.

a value of 2.6 W/mK. This calculation uses the CT dissociation front data and Equation (5) to estimate a value of 0.03 for β (a front displacement of 1.7 cm after 840 seconds). While the thermal conductivity value is clearly higher than would be expected for pure thermal conduction, it should be remembered that the value incorporates all heat-transfer processes. Hence, this lumped parameter includes advective processes and kinetic effects as well as potential experimental uncertainty, such as the effects of radial heat transport.

Conclusions

The CT images clearly track the spatial progression of a dissociation front in a sand/hydrate system. By the application of a simple moving-boundary-problem model, the advancement of the dissociation front along with applied temperature boundary conditions have been used to compute an effective thermal conductivity

for the dissociated sand/water ice system. This lumped parameter, which describes the heat-gain processes of the sand/water ice medium, is estimated as 2.6 W/m K. It is considerably higher than expected based purely upon heat conduction alone. One possible explanation for this result is that the effective thermal conductivity incorporates advective and kinetic processes associated with hydrate dissociation. Additionally, if there were significant radial heat transport into the sample, as well as end effects that the model neglects because of our assuming a semi-infinite domain, these model errors would increase the estimated thermal conductivity value. These results demonstrate the value of using remote sensing techniques to track the movement of a hydrate dissociation front for understanding the complex thermodynamics of hydrate/sand systems.

Acknowledgments

This work was supported by the Assistant Secretary for Fossil Energy, Office of Natural Gas and Petroleum Technology, through the National Energy Technology Laboratory of the U.S. Department of Energy under Contract No. DE-AC-03-76SF00098. The authors would like to thank George Moridis and Larry Myer for their support and advice conducting the CT experiment. The authors would also like to thank Jens Birkholzer for his careful review and comments.

References

Ahmadi, G., Ji, C. & Smith, D. (2000). A simple model for natural gas production from hydrate decomposition. In *Gas Hydrates, Challenges for the Future,* Annals of the New York Academy of Sciences, Vol. 912 (G.D. Holder, P.R. Bishnoi, eds.) New York.

Crank, J., (1986). *The Mathematics of Diffusion*, 2nd ed., Oxford University Press, New York, pp. 286–308.

Selim, M.S. & Sloan, E.D., (1985). Modeling of the dissociation of an in-situ hydrate, *Proceedings of the SPE 1985 California Regional Meeting*, Society of Petroleum Engineers of AIME, Bakersfield, California, pp. 75–79.

Sloan, Jr., E.D. (1998). *Clathrate Hydrates of Natural Gases*, 2nd ed., Marcel Dekker, Inc., New York.

Stern, L.A., Kirby, S.H., & Durham, W.B., (1996). Peculiarities of methane clathrate hydrate formation and solid-state deformation, including possible superheating of water ice *Science*, **273** (5283), pp. 1843–1848.

Stern, L.A., Circone, S., Kirby, S.H., & Durham, W.B. (2001). Anomolous preservation of pure methane hydrate at 1 atm, *Journal of Physical Chemistry B* **105**, 1756–1762.

Tomutsa, L., Freifeld, B.M., Kneafsey, T.J., & Stern, L.A. (2002). X-ray computed tomography observation of methane hydrate dissociation, *Proceedings of the SPE 2002 Gas Technology Symposium*, Calgary, Alberta, Canada.

Tsypkin, G.G. (2000). Mathematical models of gas hydrates dissociation in porous media. In *Gas Hydrates, Challenges for the Future,* Annals of the New York Academy of Sciences, Vol. 912, (G.D. Holder, P.R. Bishnoi, eds.) New York.

W. F. Waite, (2002). personal communication.